Nanoscale

PAPER

View Article Online
View Journal | View Issue

Published on 26 February 2014. Downloaded by Michigan State University on 20/01/2016 14:22:18.

Cite this: *Nanoscale*, 2014, **6**, 5467

Water-soluble multidentate polymers compactly coating Ag_2S quantum dots with minimized hydrodynamic size and bright emission tunable from red to second near-infrared region†

Rijun Gui,[a] Ajun Wan,*[a] Xifeng Liu,[b] Wen Yuan[c] and Hui Jin[a]

Received 16th January 2014
Accepted 24th February 2014

DOI: 10.1039/c4nr00282b

www.rsc.org/nanoscale

Hydrodynamic size-minimized quantum dots (QDs) have outstanding physicochemical properties for applications in multicolor molecular and cellular imaging at the level of single molecules and nanoparticles. In this study, we have reported the aqueous synthesis of Ag_2S QDs by using thiol-based multidentate polymers as capping reagents. By regulating the composition of the precursors ($AgNO_3$ and sulfur–$N_2H_4 \cdot H_2O$ complex) and multidentate polymers (poly(acrylic acid)-*graft*-cysteamine-*graft*-ethylenediamine), as well as the reaction time, Ag_2S QDs (2.6–3.7 nm) are prepared, displaying tunable photoluminescence (PL) emission from red to the second near-infrared region (687–1096 nm). The small hydrodynamic thickness (1.6–1.9 nm) of the multidentate polymers yields a highly compact coating for the QDs, which results in the bright fluorescent QDs with high PL quantum yields (QYs: 14.2–16.4%). Experimental results confirm that the QDs have high PL stability and ultralow cytotoxicity, as well as high PLQYs and small hydrodynamic sizes (4.5–5.6 nm) similar to fluorescent proteins (27–30 kDa), indicating the feasibility of highly effective PL imaging in cells and living animals.

1. Introduction

Previous research has disclosed that photoluminescence (PL) bioimaging in the second near-infrared region (NIR-II, 1000–1400 nm) is appealing due to the negligible scattering, minimal autofluorescence, maximal penetration depth and high feature fidelity in this region.[1–4] Compared to optical imaging of cells and live animals in the traditional near-infrared (NIR-I, 700–950 nm) and visible region (450–700 nm), earlier studies confirmed that NIR-II PL imaging is optimal due to its much lower albedo and endogenous autofluorescence, and its markedly improved signal-to-noise ratio.[5,6] During the past decade, great effort has been devoted to developing NIR-II-emitting materials for *in vivo* imaging applications. In particular, semiconductor quantum dots (QDs, such as PbS, PbSe and CdHgTe) have been prepared, but the potential toxicity from heavy-metal ions restrains their applications.[7–10] So far, the development of nontoxic, stable and bright fluorophores emitting in the NIR-II region is urgent and challenging.

Recently, silver sulfide (Ag_2S) has been widely studied due to its potential applications in photoconducting cells, photovoltaic devices and infrared detectors.[11] Particularly, nanoscaled α-Ag_2S nanocrystals (*i.e.*, Ag_2S QDs) are attractive alternatives to traditional NIR-II-emitting QDs in *in vivo* imaging because α-Ag_2S (monoclinic) has 0.85 eV of bulk bandgap.[12] Ag_2S QDs are highly biocompatible (low toxicity) because of the absence of toxic metals.[13] Moreover, Ag_2S has an ultralow solubility product constant ($K_{sp} = 6.3 \times 10^{-50}$), enabling minimal release of Ag^+ ions into the biological surroundings.[5] Wang *et al.* firstly reported a new type of NIR-II-emitting Ag_2S QDs.[14,15] Hydrophobic Ag_2S QDs were synthesized using a single source precursor of $[(C_2H_5)_2NCS_2Ag]$ in organic solvent,[14] exhibiting PL emission at 1058 nm. Through ligand exchange and chemical modification, hydrophilic Ag_2S QDs could be obtained (with emission at 1150–1200 nm).[5,16] For further applications in biosystems, the NIR-II-emitting Ag_2S QDs prepared in organic solvents[5,14–17] should undergo phase transfer from organic solvents to water, but the PL intensity, quantum yield (QY) and stability of the QDs would be compromised drastically.[18,19] Thus, the preparation of bright, stable and water-dispersible Ag_2S QDs is highly desirable.

[a]*Department of Chemistry, School of Chemistry and Chemical Engineering, Shanghai Jiao Tong University, No. 800 Dongchuan Road, Shanghai 200240, P.R. China. E-mail: wanajun@sjtu.edu.cn; Fax: +86 21 54745706; Tel: +86 21 34201245*

[b]*College of Chemistry and Chemical Engineering, Hunan University, Changsha 410082, P.R. China*

[c]*Department of Chemistry, Michigan State University, East Lansing, Michigan 48824, USA*

† Electronic supplementary information (ESI) available: Preparation of multidentate polymers (Part S1), synthetic conditions and properties of Ag_2S QDs summarized from previous synthesis methods (Table S1), EDX and XPS spectra of Ag_2S QDs (Fig. S1), photographs of Ag_2S QDs in aqueous solution under room light and excitation light (Fig. S2), analysis of Ag^+ ions leaked from Ag_2S QDs in cell culture media (Table S2), and calculation of the molar capping ratio for Ag_2S QDs (Part S2). See DOI: 10.1039/c4nr00282b

Published on 26 February 2014. Downloaded by Michigan State University on 20/01/2016 14:22:18.

Using water-soluble low-molecule-weight thiols (or Na_2S) as the S^{2-} source and $AgNO_3$ (or CH_3COOAg) as the Ag^+ source, water-dispersible Ag_2S QDs were prepared in ethylene glycol or aqueous solution.[20–25] Ag_2S QDs could be obtained under heating (90–150 °C) and even at room temperature, and the QDs were stabilized by thiols and biomolecules. Although NIR-II-emitting Ag_2S QDs can be achieved using the different methods reported previously, the PLQYs of these QDs are relatively low (<5.8%), which partly restrains their biomedical applications. As a result, further surface modification of hydrophobic QDs is widely performed to produce water-dispersible QDs.[5,16] Nevertheless, the modified procedures are relatively complicated and require strict conditions. By contrast, aqueous synthesis is straightforward, and the resultant QDs could be directly applied to biosystems without phase transfer and ligand exchange. To our knowledge, so far the Ag_2S QDs prepared in aqueous solution have a low PLQY (less than 2%). Exceptionally, Hocaoglu *et al.* recently reported the aqueous synthesis of 2-mercaptopropionic acid-capped Ag_2S QDs, showing PL emission at 780–950 nm and PLQYs of 7–39%.[25] The PLQYs are higher than other reports, but these QDs need to be incubated for several months, and the PL emission is below the NIR-II region.

Herein, we describe a facile aqueous synthesis method to prepare highly stable, bright and biocompatible Ag_2S QDs using multidentate polymers (poly(acrylic acid)-*graft*-cysteamine-*graft*-ethylenediamine) as capping reagents. Multidentate polymers were utilized not only for minimizing the hydrodynamic size of QDs but also for conquering the colloidal stability, photobleaching and PL brightness issues encountered in earlier reports.[26,27] By regulating the ratios of the precursors ($AgNO_3$ and S–$N_2H_4\cdot H_2O$) and multidentate polymers, Ag_2S QDs were achieved and possessed PL emission tunable from the red to the NIR-II region, as the reaction time is increased (10–150 min). In particular, these prepared QDs have higher PLQYs (14.2–16.4%) compared to the previously reported Ag_2S QDs. The experimental results testified that the Ag_2S QDs have high PL stability and ultralow cytotoxicity, in addition to high PLQYs and small hydrodynamic sizes similar to fluorescent proteins, implying the feasibility of using the QDs for highly effective PL imaging in cells and living animals at the level of single QDs.

2. Experimental

2.1 Chemicals and materials

$AgNO_3$ (99.9%), sulfur (S, ~200 mesh, 99.99%), hydrazine hydrate ($N_2H_4\cdot H_2O$, 99%), indocyanine green (ICG, 75%), multidentate polymers (~2.2 kDa, prepared based on ref. 26, each polymer molecule contains ~3.5 active thiols and ~3.0 amines, see Part S1 of ESI†) and bovine serum albumin (BSA, 66 kDa) were bought from Sigma-Aldrich. 3-[4,5-Dimethylthiazol-2-yl]-2,5-diphenyl-tetrazolium bromide (MTT) and other biological reagents were from Invitrogen Corp. L929 cells were obtained from the cell bank of Shanghai Science Academy of China. Other chemicals of analytical grade were purchased from Shanghai Chemical Reagent Corp. All chemicals were utilized directly as received without any purification. Ultrapure water with a resistivity of 18.2 MΩ cm^{-1} was used in the experiments. Phosphate buffered saline (PBS, 1 mM) with different pH values was prepared by regulating the molar ratio of Na_2HPO_4 and NaH_2PO_4.

2.2 Preparation of multidentate polymer-capped Ag_2S QDs

The S–$N_2H_4\cdot H_2O$ complex (as the S^{2-} source) was prepared as previously reported.[23] In detail, the S molarity (50 mM) was prepared by dissolving S powder in 85 wt% $N_2H_4\cdot H_2O$ and then diluting with water. Afterwards, multidentate polymers and $AgNO_3$ (with fixed molar ratios) were mixed in N_2 atmosphere to produce supramolecular hydrogels in water (45 mL). Next, 5 mL of the aqueous S^{2-} source was injected, and the reaction bath solution was stirred for 10–150 min at 95 °C. The resultant Ag_2S QDs were precipitated by adding acetone, collected by centrifugation, twice washed with ethanol and redispersed in water. Under different reaction times, a series of Ag_2S QDs with various sizes and PL emission wavelengths were achieved by controlling the amount of multidentate polymers and the ratio of $AgNO_3$ to S–$N_2H_4\cdot H_2O$. The QYs of Ag_2S QDs were calculated by the equation: $\Phi_s = \Phi_r (I_s/I_r) (A_r/A_s) (n_s/n_r)$, where Φ_s, I_s, A_s and n_s are the QY, emission peak area, integrated absorption intensity and refractive index of QDs, respectively, and Φ_r, I_r, A_r and n_r represent the corresponding parameters of ICG as a reference standard (13% QY, in dimethylsulfoxide).

2.3 Characterization

Absorption spectra were recorded with a UV-2450 (Shimadzu, Japan) spectrophotometer. Emission spectra were measured with an FLSP 920 (Edinburgh Instruments, U.K.) fluorescence spectrophotometer with a Xenon lamp used for excitation. Transmission electron microscopy (TEM) images and energy diffraction X-ray (EDX) were obtained on a JEOL JEM-1400 TEM instrument (JEOL, Japan) operating at an acceleration voltage of 120 kV. High resolution TEM (HRTEM) images were acquired with an H-600 (Hitachi, Japan) TEM instrument operating at an acceleration voltage of 200 kV. X-ray diffraction (XRD, Siemens, Germany) patterns were obtained with wide-angle X-ray scattering, using a D5005 X-ray powder diffractometer equipped with graphite monochromatized Cu Kα radiation (λ = 1.54056 Å). X-ray photoelectron spectroscopy (XPS, Thermon Scientific) was captured with a Kratos XSAM 800 X-ray photoelectron spectrometer. Hydrodynamic diameters were determined using dynamic light scattering apparatus (DLS, Malven Instruments, U.K.).

2.4 Measurement of stability and cytotoxicity

To study the PL stability of the Ag_2S QDs, an aqueous suspension of QDs (50 μg mL^{-1}) was incubated in 1 mM of PBS (pH 7.0) and BSA (10 mM) at 37 °C, and the PL intensities were recorded at different time intervals (0–72 h). In addition, the aqueous suspension was excited with a 405 nm laser (50 mW), and the PL intensities were measured at different time points (0–180 min). ICG molecules were selected as a reference. Briefly, ICG aqueous solution (1 μM) was excited with a 722 nm laser (50 mW), and PL intensities were recorded at different excitation times (0–180 min). To evaluate the cytotoxicity of the QDs, L929 cells were

 This journal is © The Royal Society of Chemistry 2014

Published on 26 February 2014. Downloaded by Michigan State University on 20/01/2016 14:22:18.

cultured as subconfluent monolayers on 25 cm^2 cell culture plates with vent caps in 1× minimum essential α medium supplemented with fetal bovine serum (10%) in a humidified incubator containing CO_2 (5%) at 37 °C. After grown to subconfluence, L929 cells were dissociated from the surface with trypsin solution (0.25%), and aliquots (100 μL) were seeded (1×10^4 cells) into a 96-well plate. After 24 h incubation at 37 °C, the medium was replaced with 10 μL serum-free DMEM containing Ag_2S QDs (0–1 mg mL^{-1}). These treated cells were incubated for 6–72 h at 37 °C in the dark. The cells treated with medium alone were used as the low cell death controls. Finally, the cell viabilities were quantitated by using a standard MTT assay.

2.5 Cell apoptosis and necrosis assay

L929 cells were loaded into a 6-well plate (1×10^4 cells per well). After 24 h incubation, these cells were treated with Ag_2S QDs at a concentration of 50 μg mL^{-1} for 72 h at 37 °C. Then, these cells were collected, twice washed with PBS and incubated with anti-annexin V-fluorescein isothiocyanate (FITC) and propidium iodide (PI). Single-cell suspensions were analyzed by the fluorescence activated cell sorting (FACS) within 1 h. The apoptosis and necrosis of the L929 cells induced by Ag_2S QDs were measured using an apoptosis and necrosis assay kit. Acinomycin D (0.1 μM) and H_2O_2 (1 mM) were employed as the positive controls of apoptosis and necrosis, respectively.[28]

3. Results and discussion

3.1 Synthesis and characterization of the multidentate polymer-capped Ag_2S QDs

Before this study, we reviewed related studies about the synthesis of Ag_2S QDs during the past decade. Detailed synthetic conditions and properties of the Ag_2S QDs prepared using different methods are available in the ESI (Table S1†). We found that there are very few reports referring to the aqueous synthesis of Ag_2S QDs with high PLQY (>10%). Though a 15.5% PLQY has been reported,[16] the Ag_2S QDs suffered from an intricate synthesis in organic solvents, ligand exchange and phase transfer. Another exception, 7–39% PLQYs were reported after incubating Ag_2S QDs in aqueous solution for one to several months. However, the PL emission of the QDs (780–950 nm) was below the NIR-II region.[25] Hence, the development of aqueous syntheses of Ag_2S QDs with high PLQY and NIR-II emission is significant, especially for their biomedical applications. Herein, a facile aqueous synthesis method has been put forward to prepare bright and biocompatible Ag_2S QDs by employing multidentate polymers as capping reagents, as shown in Scheme 1. Multidentate polymers help to minimize the hydrodynamic size of the QDs and overcome the colloidal stability and photobleaching. As established,[26,27] a mixed composition of –SH and $–NH_2$ groups grafted to a linear polymer chain can produce highly compact QDs with long-term colloidal stability, strong resistance to photobleaching, and a high PLQY. Multidentate polymers can wrap around QDs in a closed "loops-and-trains" conformation, which is highly stable from a thermodynamic perspective. Thus, multidentate polymers are responsible for the excellent colloidal and optical properties, and a high PLQY of the Ag_2S QDs would be expected.

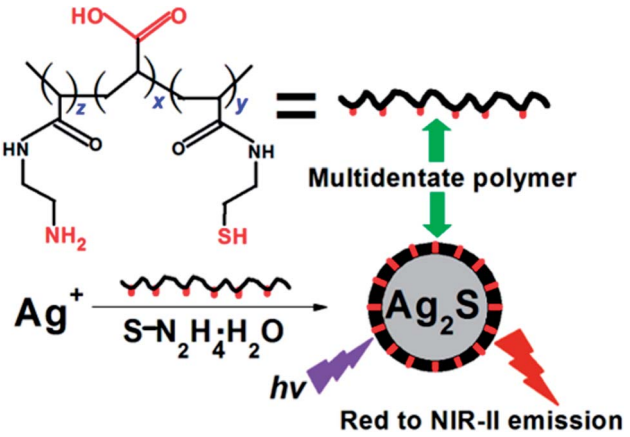

Scheme 1 Schematic illustration of the formation process of fluorescent Ag_2S QDs.

In the experiments, the multidentate polymers and Ag^+ were mixed to produce supramolecular hydrogels in aqueous solution, thus leading to the formation of Ag^+–thiolate complexes.[29] Then, the $S–N_2H_4·H_2O$ complex was added (as the S^{2-} source),[23,30] and the reaction solution was stirred for 10–150 min at 95 °C. After different reaction times, various sized Ag_2S QDs were prepared. Based on previous reports, thiol-based ligands have an intrinsic metal-chelating action, which enables them to fabricate high affinity metal–ligand clusters.[31] Due to abundant thiols existing in each multidentate polymer unit, the polymer plays a pivotal role as an excellent nucleating agent, followed by a capping agent, in the growth of the QDs.[23,26] In the absence of multidentate polymers, Ag^+ directly reacted with $S–N_2H_4·H_2O$ and rapidly generated non-fluorescent particles (>100 nm) rather than Ag_2S QDs. By controlling the reaction time, the polymer amount and the precursor ratio, Ag_2S QDs (six samples: S1 to S6) with different PL emission wavelengths and diameters were achieved. Detailed synthetic conditions and properties of the multidentate polymer-capped Ag_2S QDs are exhibited in Table 1.

During the aqueous synthesis of the Ag_2S QDs, multidentate polymers were employed to control the shape and size distribution of the QDs by preventing their uncontrolled growth and aggregation. UV-vis absorption and PL emission spectra of the products (S1–S6) are shown in Fig. 1a and b. By extending the reaction time to increase the growth of the Ag_2S QDs, both the absorption and emission spectra markedly shifted towards a longer wavelength. After 90 min of growth, the maximal PL emission of S4 appeared in the NIR-II region. S6, obtained from 150 min of continuous growth, displays typical NIR-II PL emission at 1096 nm, and their diameters were monitored by TEM (in Fig. 1c). The observed Ag_2S QDs are spherical, monodisperse and uniform with an average diameter of 3.7 nm. By reducing the concentration of multidentate polymers, the diameter of the resultant QDs increased from 2.6 to 3.7 nm (from S1 to S6). This meant that the nucleation of QDs was

Published on 26 February 2014. Downloaded by Michigan State University on 20/01/2016 14:22:18.

Table 1 Details of synthetic conditions in the preparation of Ag_2S QDs (six samples: S1–S6) with different reaction times, emission wavelengths, diameters and PLQYs

Sample number	Multidentate polymer (mM)	Ag^+ (mM)	S–$N_2H_4\cdot H_2O$ (mL)	Time (min)	Emission (nm)	Diameter from TEM/DLS (nm)	PLQY (%)
S1	10	2	5.0	10	687	2.6/4.5	14.2
S2	8	2	5.0	30	826	3.0/4.8	15.4
S3	6	2	5.0	60	942	3.3/5.0	14.7
S4	4	2	5.0	90	1002	3.5/5.3	15.5
S5	2	2	5.0	120	1037	3.6/5.4	15.9
S6	2	1	5.0	150	1096	3.7/5.3	16.4

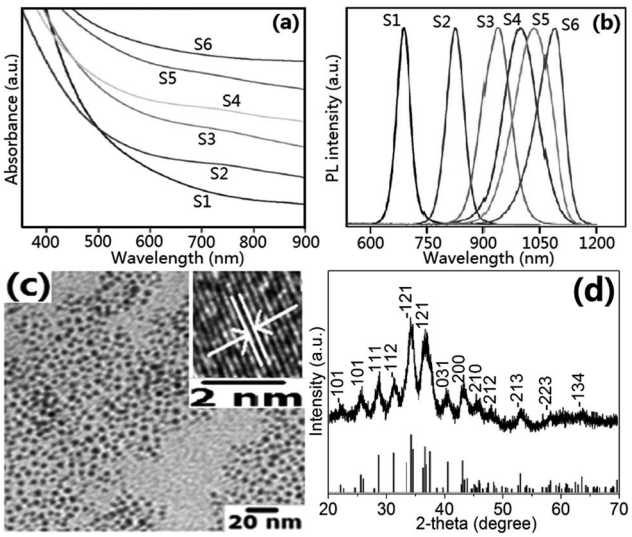

Fig. 1 (a) UV-vis absorption and (b) PL emission spectra of the Ag_2S QDs prepared under different conditions (as listed in Table 1). (c) Wide-field TEM images and local amplifying HRTEM images (inset) of the Ag_2S QDs (S6). (d) Powder XRD patterns of the Ag_2S QDs (S6) and corresponding bulk α-monoclinic Ag_2S (inset).

trapped by multidentate polymers (as capping reagents), which reduced the chance of collision and prevented the growth of the QDs.[32] At a fixed concentration of multidentate polymer, the size of the QDs increased to 3.7 nm through amplifying the ratio of S–$N_2H_4\cdot H_2O$ to Ag^+. Increasing the ratio was equal to reducing the chance of multidentate polymers combining with Ag^+, thus causing the increase in size of the QDs.[30] Increasing the size of the QDs induced the tunable PL emission, which is consistent with the quantum size effect of QDs.[33]

As shown in the inset of Fig. 1c, the crystal lattice fringes of the QDs were identified by HRTEM. The marked lattice planes indicate that the *d*-spacing of the QDs is 0.23 nm, and thus its atomic plane is indexed as the (122) facet of α-monoclinic Ag_2S,[20] The intensities and positions of the XRD peaks of the QDs are consistent with α-monoclinic Ag_2S (JCPDS card no. 65-2356), as exhibited in the inset of Fig. 1d. The diffraction peaks apparently broaden due to their nanoscale size,[34] implying the existence of Ag_2S QDs. EDX analysis (Fig. S1a, ESI†) verified the presence of Ag and S elements in the prepared products with an atomic ratio (Ag/S) of 1.73 : 1. This ratio is close to the stoichiometry of bulk Ag_2S. In the XPS spectra (Fig. S1b and c, ESI†), obvious peaks at 373.0 and 367.0 eV are assigned to the core levels of Ag $3d_{3/2}$ and Ag $3d_{5/2}$, respectively, suggesting that the oxidation state of the Ag ions is univalent in the products.[35] The two peaks (in Fig. S1b and d, ESI†) at 162.0 and 160.5 eV are assigned to the binding energies of S $2p_{1/2}$ and S $2p_{3/2}$, respectively. The spectrum of S 2p is separated by a spin-orbit splitting of 1.5 eV.[36] The actual atomic ratio (Ag/S) on the surface of the QDs is roughly 1.70 : 1, which is consistent with the EDX analysis. In addition, under room light, photographs (in Fig. S2, ESI†) of the prepared Ag_2S QDs in aqueous solution show that the color changed from transparent yellow to brown with the increase in size of the QDs. Under UV light excitation, all of the samples displayed red emission, and the size-dependent emission was observed. These photographs revealed that the Ag_2S QDs were well dispersed in aqueous solution, and there was no observable precipitation, which is ascribed to multidentate polymers effectively acting as a capping layer for preventing the agglomeration of the QDs.[23]

3.2 PLQYs and hydrodynamic sizes of the Ag_2S QDs

Fig. 2a shows that the PLQY and monodispersity of the Ag_2S QDs are dependent on the molar capping ratio (MCR),[26] calculated by dividing the sum of thiol and amine groups on the multidentate polymers by that of Ag and S atoms on the QDs surface (Part S2, ESI†). The decrease of the MCR (from 1.8 to 0.2) induces the increase of the polydispersity index (PDI),[37] which denotes that the multidentate polymers are insufficient to completely coat 3.7 nm Ag_2S QDs (S6). When the MCR is above 1.8, excess polymers induce a better size monodispersity, but a reduced PLQY. Considering both limits from the PLQY and PDI, the optimal MCR is approximately 1.8, yielding small, monodisperse QDs (PDI = 0.7) and bright fluorescence (PLQY = 16.4%). The hydrodynamic size and size distribution of S6 were analyzed by DLS. As displayed in Fig. 2b, the QDs have an average size of 5.3 ± 0.3 nm. The larger size measured from DLS (than from TEM) is ascribed to the hydrate layers in the aqueous environment,[38] further suggesting the existence of capping layers (multidentate polymers) on the surface of the Ag_2S QDs. Using the relationship in Fig. 2b, the multidentate polymer thickness was calculated to be only ~1.6 nm (for S6). The compact polymer shell results in a high degree of adsorption on the QDs surface. By contrast, the coating thickness of traditional ligands is on the order of 4–7 nm, including amphiphilic polymers and some monovalent molecular ligands.[39] In

 This journal is © The Royal Society of Chemistry 2014

Published on 26 February 2014. Downloaded by Michigan State University on 20/01/2016 14:22:18.

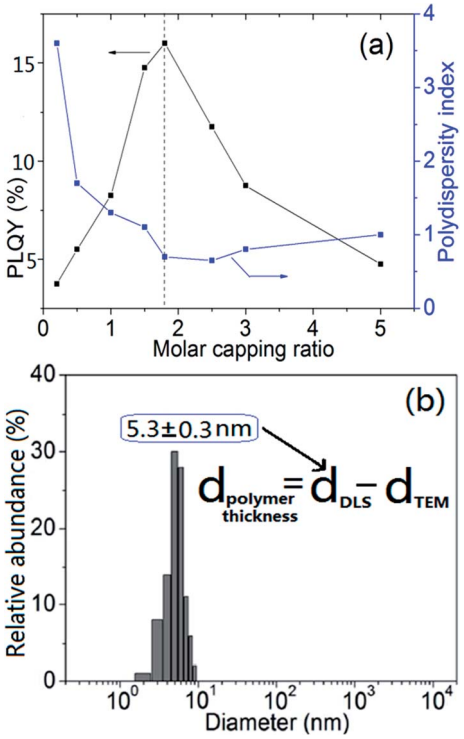

Fig. 2 (a) Effect of the multidentate polymer capping ratio on the properties of Ag_2S QDs: PLQY and polydispersity index as a function of the molar capping ratio. (b) Hydrodynamic size and size distribution of the Ag_2S QDs, and the thickness calculation of multidentate polymers on the QDs surface (inset).

previous reports, 3.3 nm Ag_2S QDs were prepared in aqueous solution employing BSA as the capping reagent, and the QDs displayed a hydrodynamic diameter ~10 nm.[6,24] In other words, the shell thickness of BSA around the QDs was ~6.7 nm. Thus, the BSA shell was not compactly coating the QDs, which is responsible for the low PLQY of QDs (1.8%). For the six samples prepared in our case (S1–S6, Table 1), the values of the polymer thickness are below 2 nm, and the hydrodynamic diameters (~5 nm) are similar to fluorescent proteins with tunable emission from the visible to NIR region.[26] In particular, these samples have relatively high PLQYs when compared to earlier reports. The hydrodynamic size-minimized Ag_2S QDs with tunable PL emission from the red to NIR-II region exhibit promising applications in multicolor molecular/cellular imaging at the level of single molecules and nanoparticles, specifically serving as an ideal NIR-II PL nanoprobe.

3.3 Stability and cytotoxicity of the Ag_2S QDs

Preceding biomedical applications of the prepared Ag_2S QDs, their PL stability and cytotoxicity should be examined first. Related experiments were conducted, and the experimental results are provided in Fig. 3. The PL stability of the Ag_2S QDs was estimated by incubating them separately in PBS and BSA at 37 °C, and the PL intensities of the QDs were recorded at different time intervals. In Fig. 3a, more than 88% of the PL was preserved after 72 h incubation, implying that the PL of the QDs is highly stable. In addition, the QDs were evaluated by

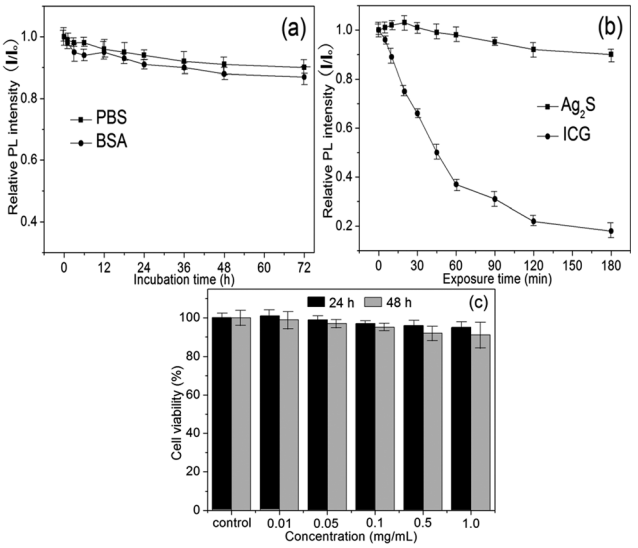

Fig. 3 (a) PL stability of the Ag_2S QDs incubated with 1 mM of PBS (pH 7.0) and BSA (10 mM) for 0–72 h at 37 °C. (b) PL stability of the Ag_2S QDs (50 μg mL^{-1}) and ICG molecules (1 μM) under continuous excitation for 0–180 min with a laser. (c) Cell viability data of L929 cells incubated with Ag_2S QDs (0–1 mg mL^{-1}) for 24 and 48 h.

continuous excitation with a 405 nm laser (50 mW). In Fig. 3b, little photobleaching (less than 10%) was observed *via* continuous excitation for 180 min, denoting that the QDs have the capacity for long-term tracking and bio-imaging. As a reference, ICG molecules as a commercial organic dye showed dramatic photobleaching. After 180 min of continuous excitation with a 722 nm laser (50 mW), ~81% photobleaching was observed. These results confirmed that the Ag_2S QDs possess high PL stability in water-soluble systems, as well as anti-photobleaching capacity. Furthermore, the cytotoxicity of the Ag_2S QDs incubated in L929 cells was also estimated by using a standard cell viability method.[19] Fig. 3c exhibits the viability of L929 cells treated with the QDs at different incubation times (24 and 48 h). At a concentration of 1 mg mL^{-1}, the QDs generated negligible effects on the cell viability, and a cell viability of more than 91% remained after 48 h incubation with the QDs. In addition, during the incubation in cell culture media, the leakage of Ag^+ ions from the Ag_2S QDs as a function of the incubation time was analyzed. The experimental results (Table S2, ESI†) indicated that a neglectable amount (<1%) of Ag^+ ions leaked from the Ag_2S QDs were detected. The extremely low leakage of toxic Ag^+ ions into cells was responsible for the high viability of the cells treated with the Ag_2S QDs. According to the above results, when swallowed by tumor cells, the QDs could be considered as safe nanoprobes used for *in vivo* PL imaging of living small animals.

3.4 Cell apoptosis and necrosis induced by the Ag_2S QDs

The above results revealed the high PL stability and favorable cytotoxicity of the Ag_2S QDs, thus showing a promising application as NIR-II nanoprobes. To further investigate their biocompatibility, related experiments were performed. Typically, annexin V-FITC staining and PI incorporation were

Published on 26 February 2014. Downloaded by Michigan State University on 20/01/2016 14:22:18.

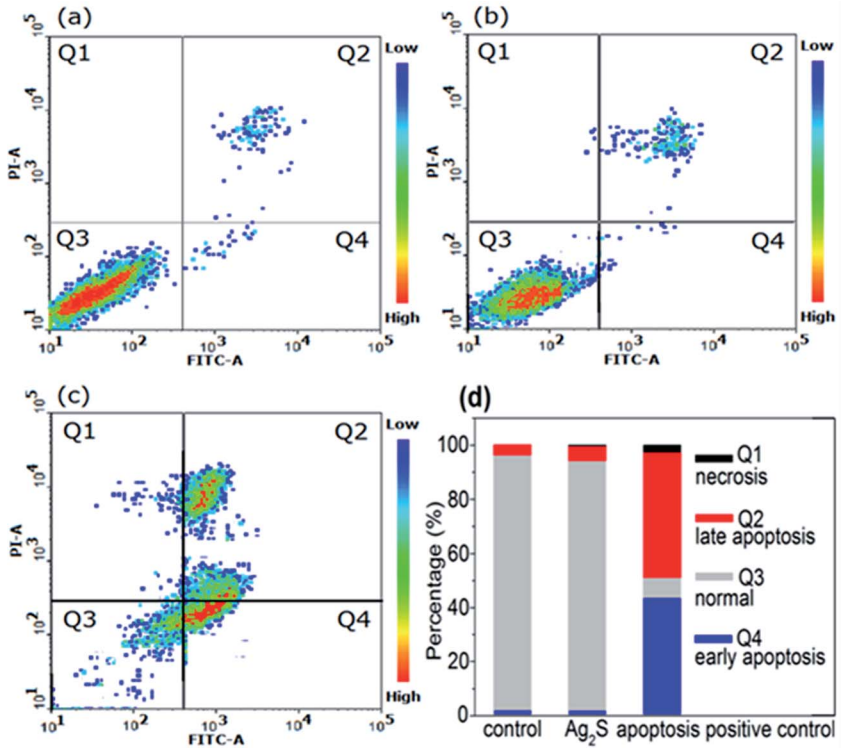

Fig. 4 Apoptosis and necrosis of L929 cells induced by the Ag_2S QDs after 72 h treatment. (a) Apoptosis positive control of acinomycin D (0.1 μM). (b) FACS plot with 1.0 mg mL^{-1} Ag_2S QDs. (c) Necrosis positive control of H_2O_2 (1 mM). (d) Quantitative flow cytometry results.

carried out to estimate the L929 cellular apoptosis and necrosis induced by the Ag_2S QDs. As elaborated in Fig. 4, after 72 h treatment of cells with the QDs, flow cytometry data from the induced apoptosis and necrosis on the L929 cells illustrated that the QDs had negligible cytotoxicity. In the FACS dot plot, each dot represents an individual cell. In Fig. 4a–c, the cells appearing in the upper left quadrant (Q1) represent the necrosis cells, and the cells appearing in the lower left quadrant (Q3) denote the normal cells. In addition, those appearing in the upper right quadrant (Q2) and in the lower right quadrant (Q4) represented these cells in the late and early stages, respectively. With a concentration of the Ag_2S QDs of 1.0 mg mL^{-1}, the population of L929 cells (in Fig. 4b) that underwent apoptosis and necrosis remained nearly unchanged, and there was no marked difference in comparison to the apoptosis positive control without Ag_2S QDs (in Fig. 4a). In the necrosis positive control (Fig. 4c), the proportions of Q1, Q2 and Q4 were significantly larger than the group of QDs and the apoptosis positive control, exhibiting a remarkable cytotoxicity. These results further suggest that the Ag_2S QDs have negligible cytotoxicity and excellent biocompatibility even at a concentration of up to 1.0 mg mL^{-1} in tumor cells.

4. Conclusions

In summary, we demonstrated a facile aqueous synthesis of Ag_2S QDs with bright and tunable PL emission from the red to NIR-II region, employing multidentate polymers as capping reagents. By adjusting the concentration of multidentate polymers and the ratio of the precursors ($AgNO_3$ and $S–N_2H_4·H_2O$), various nano-scaled Ag_2S QDs were prepared under different reaction times. These prepared Ag_2S QDs (2.6–3.7 nm) displayed PL emission from 687 to 1096 nm. The hydrodynamic thickness from the multidentate polymers on the surface of the QDs is only ~2 nm, yielding a highly compact coating on the QDs. The small thickness of the polymers resulted in the bright PL of the QDs with relatively high PLQYs (14.2–16.4%) compared to previous reports. In addition to the high PLQYs and small hydrodynamic diameters (4.5–5.6 nm) similar to fluorescent proteins, these Ag_2S QDs presented high PL stability, ultralow cytotoxicity and excellent biocompatibility. These favorable properties indicated the feasibility of using the QDs for highly effective PL imaging in cells and living animals, especially for multicolor molecular and cellular imaging at the level of single molecules and QDs.

Acknowledgements

This work was supported by grants from the National Natural Science Foundation of China (no. 51173104), the Nanotechnology Program of Science and Technology Committee of Shanghai (no. 11nm0503500), and the Postdoctoral Science Foundation of China (no. 2013M531164) and Shanghai (no. 13R21413800).

References

1 K. Welsher, Z. Liu, S. P. Sherlock, J. T. Robinson, Z. Chen, D. Daranciang and H. Dai, *Nat. Nanotechnol.*, 2009, **4**, 773–780.

 This journal is © The Royal Society of Chemistry 2014

Published on 26 February 2014. Downloaded by Michigan State University on 20/01/2016 14:22:18.

2 Z. Liu, S. Tabakman, K. Welsher and H. Dai, *Nano Res.*, 2009, **2**, 85–120.
3 A. M. Smith, M. C. Mancini and S. M. Nie, *Nat. Nanotechnol.*, 2009, **4**, 710–711.
4 K. Welsher, S. P. Sherlock and H. Dai, *Proc. Natl. Acad. Sci. U. S. A.*, 2011, **108**, 8943–8948.
5 Y. Zhang, G. Hong, Y. Zhang, G. Chen, F. Li, H. Dai and Q. Wang, *ACS Nano*, 2012, **6**, 3695–3702.
6 H. Y. Yang, Y. W. Zhao, Z. Y. Zhang, H. M. Xiong and S. N. Yu, *Nanotechnology*, 2013, **24**, 055706.
7 L. Bakueva, I. Gorelikov, S. Musikhin, X. S. Zhao, E. H. Sargent and E. Kumacheva, *Adv. Mater.*, 2004, **16**, 926–929.
8 B. L. Wehrenberg, C. Wang and P. Guyot-Sionnest, *J. Phys. Chem. B*, 2002, **106**, 10634–10640.
9 M. T. Harrison, S. V. Kershaw, M. G. Burt, A. Eychmuller, H. Weller and A. L. Rogach, *Mater. Sci. Eng., B*, 2000, **69**, 355–360.
10 P. Zrazhevskiy, M. Senawb and X. Gao, *Chem. Soc. Rev.*, 2010, **39**, 4326–4354.
11 K. Akamatsu, S. Takei, M. Mizuhata, A. Kajinami, S. Deki, S. Takeoka, M. Fujii, S. Hayashi and K. Yamamoto, *Thin Solid Films*, 2000, **359**, 55–60.
12 M. Yarema, S. Pichler, M. Sytnyk, R. Seyrkammer, R. T. Lechner and G. Fritz-Popovski, *ACS Nano*, 2011, **5**, 3758–3765.
13 B. Nowack, *Science*, 2010, **330**, 1054–1055.
14 Y. Du, B. Xu, T. Fu, M. Cai, F. Li, Y. Zhang and Q. Wang, *J. Am. Chem. Soc.*, 2010, **132**, 1470–1471.
15 S. Shen, Y. J. Zhang, L. Peng, Y. Du and Q. Wang, *Angew. Chem., Int. Ed.*, 2011, **50**, 7115–7118.
16 G. Hong, J. T. Robinson, Y. Zhang, S. Diao, A. L. Antaris, Q. Wang and H. Dai, *Angew. Chem., Int. Ed.*, 2012, **51**, 9818–9821.
17 P. Jiang, Z. Q. Tian, C. N. Zhu, Z. L. Zhang and D. W. Pang, *Chem. Mater.*, 2012, **24**, 3–5.
18 A. Sahu, L. Qi, M. S. Kang, D. Deng and D. J. J. Norris, *J. Am. Chem. Soc.*, 2011, **133**, 6509–6512.
19 C. Chen, X. He, L. Gao and N. Ma, *ACS Appl. Mater. Interfaces*, 2013, **5**, 1149–1155.
20 P. Jiang, C. N. Zhu, Z. L. Zhang, Z. Q. Tian and D. W. Pang, *Biomaterials*, 2012, **33**, 5130–5135.
21 L. Tan, A. Wan and H. Li, *Langmuir*, 2013, **29**, 15032–15042.
22 L. Tan, A. Wan and H. Li, *ACS Appl. Mater. Interfaces*, 2013, **5**, 11163–11171.
23 C. Wang, Y. Wang, L. Xu, D. Zhang, M. Liu, X. Li, H. Sun, Q. Lin and B. Yang, *Small*, 2012, **8**, 3137–3142.
24 Y. Wang and X. P. Yan, *Chem. Commun.*, 2013, **49**, 3324–3326.
25 I. Hocaoglu, M. N. Cizmeciyan, R. Erdem, C. Ozen, A. Kurt, A. Sennaroglu and H. Y. Acar, *J. Mater. Chem.*, 2012, **22**, 14674–14681.
26 A. M. Smith and S. Nie, *J. Am. Chem. Soc.*, 2008, **130**, 11278–11279.
27 L. Liu, X. Guo, Y. Li and X. Zhong, *Inorg. Chem.*, 2010, **49**, 3768–3775.
28 H. Yang, Z. Rivera, S. Jube, M. Nasu, P. Bertino, C. Goparaju, G. Franzoso, M. T. Lotze, T. Krausz and H. I. Pass, *Proc. Natl. Acad. Sci. U. S. A.*, 2010, **107**, 12611–12616.
29 J. S. Shen, D. H. Li, Q. G. Cai and Y. B. Jiang, *J. Mater. Chem.*, 2009, **19**, 6219–6224.
30 M. N. Kalasad, M. K. Rabinal and B. G. Mulimani, *J. Phys. D: Appl. Phys.*, 2010, **43**, 305301.
31 C. Zhou, M. Long, Y. P. Qin, X. K. Sun and J. Zheng, *Angew. Chem., Int. Ed.*, 2011, **50**, 3168–3172.
32 Y. Negishi, K. Nobusada and T. Tsukuda, *J. Am. Chem. Soc.*, 2005, **127**, 5261–5270.
33 C. C. Huang, Z. Yang, K. H. Lee and H. T. Chang, *Angew. Chem., Int. Ed.*, 2007, **46**, 6824–6828.
34 V. Nandwana, K. E. Elkins, N. Poudyal, G. S. Chaubey, K. Yano and J. P. Liu, *J. Phys. Chem. C*, 2007, **111**, 4185–4189.
35 J. Xiang, H. Cao, Q. Wu, S. Zhang, X. Zhang and A. A. R. Watt, *J. Phys. Chem. C*, 2008, **112**, 3580–3584.
36 B. Zhang, X. Ye, W. Dai, W. Hou and Y. Xie, *Chem. - Eur. J.*, 2006, **12**, 2337–2342.
37 B. Chu, Z. Wang and J. Yu, *Macromolecules*, 1991, **24**, 6832–6838.
38 C. Liu, J. Guo, W. Yang, J. Hu, C. Wang and S. Fu, *J. Mater. Chem.*, 2009, **19**, 4764–4770.
39 T. Pons, H. T. Uyeda, I. L. Medintz and H. Mattoussi, *J. Phys. Chem. B*, 2006, **110**, 20308–20316.